Universal $d = 1$ flat band generator from compact localized states

Wulayimu Maimaiti,[1,2] Sergej Flach,[1] and Alexei Andreanov[1]
[1]*Center for Theoretical Physics of Complex Systems, Institute for Basic Science (IBS), Daejeon 34126, Republic of Korea*
[2]*Basic Science Program, Korea University of Science and Technology (UST), Daejeon 34113, Republic of Korea*

(Received 25 October 2018; published 18 March 2019)

The band structure of some translationally invariant lattice Hamiltonians contains strictly dispersionless flat bands (FB). These are induced by destructive interference and typically host compact localized eigenstates (CLS) which occupy a finite number U of unit cells. FBs are important due to macroscopic degeneracy and consequently due to their high sensitivity and strong response to different types of weak perturbations. We use a recently introduced classification of FB networks based on CLS properties, and extend the FB Hamiltonian generator introduced in Phys. Rev. B **95**, 115135 (2017) to an arbitrary number ν of bands in the band structure, and arbitrary size U of a CLS. The FB Hamiltonian is a solution to equations that we identify with an inverse eigenvalue problem. These can be solved only numerically in general. By imposing additional constraints, e.g., a chiral symmetry, we are able to find analytical solutions to the inverse eigenvalue problem.

DOI: 10.1103/PhysRevB.99.125129

I. INTRODUCTION

Physical models featuring macroscopically degenerate eigenstates have attracted a lot of attention in the past decades. Such degeneracies are naturally unstable to slightest perturbations making them perfect candidates for exotic or unconventional correlated phases of matter like in frustrated magnetism, and strongly correlated systems. An active field in this direction is the understanding of properties of flat bands (FB), i.e., bands with no dispersion [1,2]. FB models are usually translationally invariant tight-binding networks which are characterized by a certain hopping connectivity between different network sites and which characterize the wave function of, e.g., a quantum particle, a macroscopic condensate, or a photonic field in a structured medium. [2,3] The band structure of the corresponding eigenvalue problem contains ν bands if the unit cell of the network is containing ν sites. FB networks were widely studied theoretically in lattice dimension $d = 1$ [4–6], $d = 2$ [7–9], and $d = 3$ [7,10–15]. FBs have been experimentally realized in a variety of setups, including optical wave guide networks, exciton-polariton condensates, and ultracold atomic condensates [16–24].

The absence of dispersion in FBs happens due to destructive interference. Destructive interference is also the cause of the existence of *compact localized states* (CLS). CLS are eigenstates at the FB energy, that have strictly finite support on the lattice, and occupy a finite number U of unit cells. Since any translation of a CLS is necessarily again an eigenstate for a translationally invariant Hamiltonian, the existence of a CLS is a direct proof of existence of an FB and its macroscopic degeneracy.

System perturbations typically destroy CLS leading to a variety of interesting phenomena: flat band ferromagnetism in the fermionic Hubbard model [7,8,12,25–28], energy dependent scaling of disorder-induced localization length [29], singular mobility edges with quasiperiodic potentials [30,31], Landau-Zener Bloch oscillations in the presence of external fields [32], discrete breathers in nonlinear flat band lattices [33–35], pair formation of hard core bosons [36], and geometric origin of superfluidity [37,38]. Several approaches were developed to construct FB networks: line graph constructions [7], decorated lattices [8], origami rules [39], repetition of miniarrays [40], chiral symmetry based ones [15], and methods based on local symmetries of the Hamiltonian [41]. Nishino *et al.* [10,42] used specific CLS and network symmetries to fine-tune the hoppings down to a FB.

A systematic classification of FBs in terms of compact localized states was introduced in Ref. [43], where FBs are classified by the size U of the CLS: the number of unit cells occupied by CLS. CLS-based FB generators were then obtained for $U = 1$ and arbitrary number of bands and dimension [43] covering all FB models of that class. For $\nu = 2$ and $U = 2$ in one dimension, a generator was obtained in Ref. [44] describing all the possible $d = 1$ FB networks with two bands. These FB networks form a two-parameter family of generalized sawtooth chains.

In this work, we focus on the case $d = 1$ deferring higher dimensions, where we expect even richer phenomenology, for future work. The $d = 1$ case was so far analyzed only for two bands and $U = 2$ [44]. Many recent theoretical proposals [40,45–51] and experimental attempts of realizations [18,19,24,52] focus on $d = 1$ settings, and make it necessary to obtain firstly an as complete as possible evaluation of the general $d = 1$ case.

We extend the $\nu = 2$ flat band generator [44] approach to any value of ν and U. The paper is organized as follow. In Sec. II, we provide the main definitions that we are using throughout the paper. Section III A discusses the relationship between the FB Hamiltonians and the inverse eigenvalue problems. That relationship is turned into an efficient FB generator in Sec. III B. In Sec. IV, we present the solutions for the FB generator. We conclude by summarising our results and discussing open problems.

II. MAIN DEFINITIONS

In this work, we consider a one-dimensional ($d = 1$) translationally invariant lattice Hamiltonian with $\nu > 1$ lattice sites per unit cell. We label unit cells by the index n, so that the full wave function reads $\Psi = (\ldots, \vec{\psi}_{n-1}, \vec{\psi}_n, \ldots)$. Here individual vectors $\vec{\psi}_n$ have elements ψ_{nm}, $m = 1, \ldots \nu$ labels sites inside the unit cell. Consequently the complex amplitude on the mth site in the nth unit cell reads as ψ_{nm}. We will use the notation $\vec{\psi}_n$ for the wave functions along with the bra-ket notation, $|\psi_n\rangle$, throughout the paper.

Any translationally invariant Hamiltonian can be characterized by a set of hopping matrices H_m, $m = 0, 1, \ldots$, where H_0 is the intracell hopping, H_1 describes nearest-neighbor unit cell hopping, etc. The case of finite-range hopping is additionally characterized by m_c (the maximum range of the hopping). For the sake of simplicity, we restrict our analysis to the simplest case of $m_c = 1$. Most of the results presented below carry over to the cases of $m_c > 1$ with minimal changes, that we indicate in the text, where appropriate. We restrict the analysis to the case of a single flat band in the system, and postpone the more general case of multiple flat bands for later studies.

With the above conventions and notations the eigenvalue problem for an arbitrary nearest-neighbor Hamiltonian reads [44]

$$H_1^\dagger \vec{\psi}_{l-1} + H_0 \vec{\psi}_l + H_1 \vec{\psi}_{l+1} = E \vec{\psi}_l, \quad l \in \mathbb{Z}. \tag{1}$$

The Hamiltonian of the system is a tridiagonal block matrix

$$\mathcal{H} = \begin{pmatrix} \ddots & \ddots & 0 & 0 & \ldots & 0 & 0 & \ldots \\ \ddots & H_0 & H_1 & 0 & 0 & \ldots & 0 & \ldots \\ 0 & H_1^\dagger & H_0 & H_1 & 0 & \ldots & 0 & \ldots \\ \ldots & 0 & \ddots & \ddots & \ddots & \ddots & \vdots & \ldots \\ \ldots & \vdots & \ldots & 0 & H_1^\dagger & H_0 & H_1 & 0 \\ \ldots & 0 & \ldots & 0 & 0 & H_1^\dagger & H_0 & \ddots \\ \ldots & 0 & 0 & \ldots & 0 & 0 & \ddots & \ddots \end{pmatrix}. \tag{2}$$

Compact localized state. A CLS is an eigenvector of (1) with $\vec{\psi}_n \neq 0$ only for a strictly finite number U of adjacent unit cells and zero everywhere else [43]. The value U is referred to as the *class* of CLS. The presence of a CLS in the spectrum of a translationally invariant Hamiltonian implies an FB. Indeed, in the infinite lattice size limit, infinitely many discrete translations of a CLS will be linearly independent. A CLS with a larger size $V > U$ can be generated from a given class U CLS by linear superpositions. Therefore the class U refers to the irreducible smallest value of U for which a CLS can not be represented as a linear superposition of even smaller CLS for a given FB network/Hamiltonian. As far as we can tell, for all known translationally invariant flat band Hamiltonians with finite range hoppings, the FB eigenspace does decompose into a CLS set. For the translationally invariant $d = 1$ case the set of all CLS forms a complete basis [44]. The eigenenergy of a flat band will be denoted as E_{FB}.

The CLS is an eigenvector $\Psi_{\mathrm{CLS}} = (\vec{\psi}_1, \vec{\psi}_2, \ldots \vec{\psi}_U)$ of the $U \times U$ block matrix

$$\mathcal{H}_U = \begin{pmatrix} H_0 & H_1 & 0 & 0 & \ldots & 0 \\ H_1^\dagger & H_0 & H_1 & 0 & \ldots & 0 \\ 0 & \ddots & \ddots & \ddots & \ddots & \vdots \\ \vdots & & & & & \vdots \\ 0 & \ldots & 0 & H_1^\dagger & H_0 & H_1 \\ 0 & \ldots & 0 & 0 & H_1^\dagger & H_0 \end{pmatrix} \tag{3}$$

with eigenenergy E_{FB}. Additionally the CLS has to satisfy the destructive interference (compactness) conditions

$$H_1 \vec{\psi}_1 = H_1^\dagger \vec{\psi}_U = 0, \tag{4}$$

that ensure that the wave function amplitudes vanish everywhere except for the U unit cells occupied by Ψ_{CLS}.[1] Therefore a *necessary* condition for the existence of a CLS reads

$$\det H_1 = 0. \tag{5}$$

Chiral symmetry. An important subclass of FB networks is that with chiral symmetry. [15] Chiral lattices are bipartite networks with minority and a majority sublattices. This imposes a specific structure of the hopping integrals and the CLS amplitudes $\vec{\psi}_l$. For that we split the lattice sites from each unit cell into two subsets, each belonging to one of the two sublattices. This leads to a splitting of each $\vec{\psi}_l$ into two sublattice vectors, as well as to a corresponding block structure of the matrices H_0, H_1. As a result the CLS of a chiral flat band will always reside exclusively on the majority sublattice [15]:

$$H_0 = \begin{pmatrix} 0 & A^\dagger \\ A & 0 \end{pmatrix}, \quad H_1 = \begin{pmatrix} 0 & T^\dagger \\ S & 0 \end{pmatrix},$$
$$\vec{\psi}_l = \begin{pmatrix} \vec{\varphi}_l \\ 0 \end{pmatrix}, \quad l = 1, \ldots, U. \tag{6}$$

Here, A, S, and T are $(\nu - \mu) \times \mu$ matrices, μ is the number of sites on the majority sublattice in the unit cell, and $\vec{\varphi}_l$ is a μ component vector residing on the majority sublattice sites in a unit cell. By definition $\nu - \mu \leqslant \mu < \nu$. The spectrum of the system enjoys particle-hole symmetry around $E = 0$. A chiral flat band has energy $E_{\mathrm{FB}} = 0$ and is symmetry protected. For $\nu < 2\mu$, there are $\mu - \lfloor \nu/2 \rfloor$ flat bands at $E_{\mathrm{FB}} = 0$ [15]. Increasing the range of hopping $m_c > 1$ while preserving the chiral symmetry will keep the chiral flat bands in place. Moreover one can keep the chiral flat bands by partially destroying the chiral and sublattice symmetry. This is achieved by adding hopping terms on the minority sublattice only, since the chiral FB CLS is occupying majority sublattice sites only:

$$H_0 = \begin{pmatrix} 0 & A^\dagger \\ A & B \end{pmatrix}, \quad H_1 = \begin{pmatrix} 0 & T^\dagger \\ S & W \end{pmatrix},$$
$$\vec{\psi}_l = \begin{pmatrix} \vec{\varphi}_l \\ 0 \end{pmatrix}, \quad l = 1, \ldots, U. \tag{7}$$

[1] In the presence of longer-range hopping $m_c > 1$, the CLS compactness conditions become more involved [44]

where B and W are $(\nu - \mu) \times (\nu - \mu)$ matrices. Note that the overall particle-hole symmetry of the system is lost, but the original chiral flat bands are still present at $E_{\rm FB} = 0$.

III. THE FLAT BAND GENERATOR

The flat band generator introduced below is based on a generalization of the concept developed in Ref. [44] for $\nu = U = 2$.

A. Inverse eigenvalue problem

We rewrite the CLS problem [(3) and (4)] as

$$H_1\vec{\psi}_2 = (E_{\rm FB} - H_0)\vec{\psi}_1, \tag{8}$$

$$H_1^\dagger\vec{\psi}_{l-1} + H_1\vec{\psi}_{l+1} = (E_{\rm FB} - H_0)\vec{\psi}_l,\ 2 \leqslant l \leqslant U-1, \tag{9}$$

$$H_1^\dagger\vec{\psi}_{U-1} = (E_{\rm FB} - H_0)\vec{\psi}_U, \tag{10}$$

$$H_1\vec{\psi}_1 = H_1^\dagger\vec{\psi}_U = 0, \tag{11}$$

$$\vec{\psi}_l = 0,\ l < 0,\ l > U. \tag{12}$$

This set of equations is the starting point of our flat band generator. Our goal is to generate all possible matrices H_1 which allow for the existence of a flat band, given a particular choice of H_0. Note that H_0 can be diagonal (canonical form), but any nondiagonal Hermitian choice of H_0 is fine as well.

One way to look for solutions is to parametrize H_1 and to compute the flat band energy $E_{\rm FB}$ and the CLS $\Psi_{\rm CLS}$ for a given set of U and ν. In order to satisfy (11), we choose H_1 from the space $\mathcal{Z}$ of $\nu \times \nu$ matrices with one zero eigenvalue. Then the directions of the vectors $\vec{\psi}_1$, $\vec{\psi}_U$ are fixed by the choice of H_1, leaving their two norms as free variables. Together with the remaining unknown CLS components and the flat band energy we arrive at $V = (U-2)\nu + 3$ variables. The total number of equations from (8)–(10) is $E = U\nu$. Since $\nu \geqslant 2$ it follows that the set of equations is overdetermined. We need $2\nu - 3$ additional constraints which will lead us to the proper codimension $(2\nu - 3)$ manifold in the space $\mathcal{Z}$. For $\nu = 2$, the codimension (1) manifold was computed explicitly and a closed form of the functional dependence of the CLS and flat band energy on H_1 was obtained in Ref. [44]. For larger values of ν (and U), the constraint computation turns hard. Therefore we will simply invert the approach—we will define the CLS (thereby setting U) and $E_{\rm FB}$ and generate the proper H_1 matrix manifold. This will turn an overcomplete set of equations into an undercomplete one, which is easier to be analyzed.

Let us assume that ψ_1 is not orthogonal to ψ_U. Multiplying $\langle\psi_U|$ from the left with equation (8), the flat band energy $E_{\rm FB}$ follows as[2]

$$E_{\rm FB} = \frac{\langle\psi_U|H_0|\psi_1\rangle}{\langle\psi_1|\psi_U\rangle}. \tag{13}$$

[2]For $m_c > 1$, one has to assume $H_m, m < m_c$ are also input parameters.

For practical purposes, we can choose the CLS normalization condition $\langle\psi_1|\psi_U\rangle = 1$. Note that if ψ_1 is orthogonal to ψ_U, the CLS class is reduced to a $U-1$ class by an appropriate unitary transformation including a redefinition of the unit cell (see Appendix A).

We can then treat the problem of flat band generation (8)–(12) as an inverse eigenvalue problem [53]: given $E_{\rm FB}$ and $\Psi_{\rm CLS}$—as well as part of the Hamiltonian—H_0, we reconstruct the Hamiltonian matrix $\mathcal{H}$, Eq. (2). The idea of finding hopping matrices for a fixed CLS was first introduced by Nishino, Goda, and Kusakabe [10,42]. Our results, even if limited to $d = 1$ in the present work, are much more systematic: compared the work of Nishino, Goda, and Kusakabe, we classify CLS by their size U, introduce the constraints on $\Psi_{\rm CLS}$ ensuring that it is a U-class CLS and show how to resolve these constraints.

B. The generator

We arrive at the following algorithm to construct a Hamiltonian with a flat band from a given CLS.

(1) Fix the number of bands ν and the size of the CLS U.

(2) Choose H_0, either as a diagonal (canonical form), or as any Hermitian matrix.

(3) Choose a real $E_{\rm FB}$.

(4) Choose $\vec{\psi}_1$ (or $\vec{\psi}_U$).

(5) Exclude H_1 from (8)–(12), arrive at a set of two linear and further nonlinear constraints, and solve them for the remaining CLS components $\vec{\psi}_l$.

(6) Solve the linear system (8)–(12) to find H_1.

The system (8)–(12) is linear, and therefore it is easy to solve it, or to show that it has no solution. Typically, if this system has a solution, it will be undercomplete and show up with multiple solutions compatible with the input CLS. It is therefore enough to find a *particular* solution $\bar{H}_1$ to Eqs. (8)–(12). A generic solution $H_1 = \bar{H}_1 + \delta H_1$, where δH_1 follows from the homogeneous system of equations:

$$\begin{gathered}
\delta H_1\vec{\psi}_2 = 0,\\
\delta H_1^\dagger\vec{\psi}_{l-1} + \delta H_1\vec{\psi}_{l+1} = 0, \quad 2 \leqslant l \leqslant U-1,\\
\delta H_{U-1}^\dagger\vec{\psi}_{U-1} = 0,\\
\delta H_1\vec{\psi}_1 = \delta H_1^\dagger\vec{\psi}_U = 0,\\
\vec{\psi}_l = 0 \quad l < 0,\ l > U.
\end{gathered} \tag{14}$$

The perturbation δH_1 is a deformation of the Hamiltonian $\mathcal{H}$ which preserves the CLS and the flat band energy and only affects the dispersive part of the spectrum.

It is also possible to further constrain the network connectivity by choosing specific elements of H_0 and/or H_1 to be zero. This is easily accounted for in H_0, which is an input parameter. The case of H_1 is more involved as discussed in Sec. IV B.

IV. SOLUTIONS

We proceed to classify flat bands in the order of increasing U. The $U = 1$ case has already been completed in Ref. [43], therefore we start our classification with $U = 2$.

A. $U = 2$

We fix the number of bands to ν, and choose some H_0, $E_{\rm FB}$, and $|\psi_1\rangle$. The inverse eigenvalue problem Eqs. (8)–(12) now reads

$$\begin{aligned} H_1|\psi_2\rangle &= (E_{\rm FB} - H_0)|\psi_1\rangle, \\ \langle\psi_1|H_1 &= \langle\psi_2|(E_{\rm FB} - H_0), \\ H_1|\psi_1\rangle &= 0, \\ \langle\psi_2|H_1 &= 0. \end{aligned} \tag{15}$$

The eigenfunction $\Psi_{\rm CLS} = (\vec{\psi}_1, \vec{\psi}_2)$ cannot be chosen arbitrarily—its second part $|\psi_2\rangle$ has to satisfy the following set of linear and nonlinear compatibility constraints:

$$\begin{aligned} \langle\psi_1|\psi_2\rangle &= 1, \\ \langle\psi_1|H_0|\psi_2\rangle &= E_{\rm FB}, \\ \langle\psi_1|E_{\rm FB} - H_0|\psi_1\rangle &= \langle\psi_1|E_{\rm FB} - H_0|\psi_1\rangle. \end{aligned} \tag{16}$$

The first constraint is simply a choice of normalization of $\Psi_{\rm CLS}$. The second constraint follows from Eq. (13) and uses $E_{\rm FB}$ as input variable. The last identity results from multiplying the first equation in Eqs. (15) by $\langle\psi_2|$ from the left, and multiplying the second equation in Eqs. (15) by $|\psi_1\rangle$ from the right. It is not possible to solve the third constraint analytically in general, but we present in Appendix C 1 a numerical algorithm that allows to resolve these constraints and enumerate all the solutions, if existing. If existing, the solution to $|\psi_2\rangle$ has $\nu - 3$ free parameters. For the special case of two bands $\nu = 2$, the flat band energy $E_{\rm FB}$ can not be chosen arbitrarily and needs to be included into the procedure as a to be defined variable. Note that this particular case can be solved in closed analytical form following a different solution strategy [44].

Once $\Psi_{\rm CLS} = (\vec{\psi}_1, \vec{\psi}_2)$ is known, we can solve Eq. (15) for H_1. First we note that the last two equations - the destructive interference conditions—can be taken into account with the following *Ansatz* for H_1:

$$H_1 = Q_2\, M\, Q_1, \quad Q_i = \mathbb{I} - \frac{|\psi_i\rangle\langle\psi_i|}{\langle\psi_i||\psi_i\rangle}. \tag{17}$$

Then Eq. (15) becomes an inverse eigenvalue problem. The details of the derivation are presented in Appendix B and the solution is

$$\begin{aligned} H_1 &= G_1 + \delta H_1, \\ G_1 &= \frac{(E_{\rm FB} - H_0)|\psi_1\rangle\langle\psi_2|(E_{\rm FB} - H_0)}{\langle\psi_1|E_{\rm FB} - H_0|\psi_1\rangle}, \\ \delta H_1 &= Q_{12}\, K\, Q_{12}, \end{aligned} \tag{18}$$

where K is an arbitrary $\nu \times \nu$ matrix and Q_{12} is a joint transverse projector on $|\psi_1\rangle, |\psi_2\rangle$: $Q_{12}|\psi_i\rangle = 0$, $i = 1, 2$. If the denominator $\langle\psi_1|E_{\rm FB} - H_0|\psi_1\rangle \equiv 0$, the above solution is replaced with a more complicated expression involving two different projectors (see Appendix B for details).

It is instructive to count the number F of free parameters in the above solution, given a fixed H_0, $E_{\rm FB}$ and $|\psi_1\rangle$ for $\nu \geqslant 3$. It is the sum of two contributions: the number of free parameters in δH_1 and in the particular solution G_1, which are $(\nu - 2)^2$ and $(\nu - 3)$ respectively. The final result is $F = \nu^2 - 3\nu + 1$.

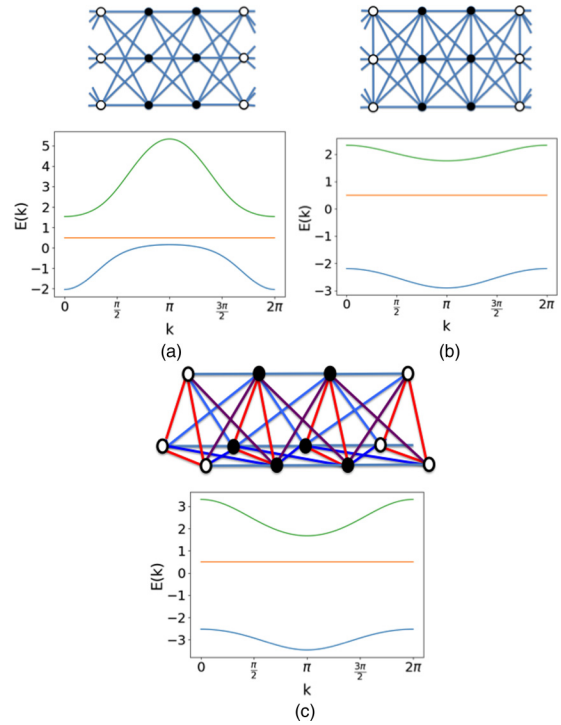

FIG. 1. Examples of flat band Hamiltonians with CLS of class $U = 2$, $\nu = 3$. The sites occupied by a CLS are indicated by filled black circles. Each subfigure contains the visualization of the lattice (top) and the band structure (bottom). The flat band is colored in orange. (a) Diagonal H_0, (b) nondiagonal H_0, and (c) nondiagonal and fully connected H_0. Appendix D 1 contains the detailed description of the Hamiltonians.

It then follows that the flat band Hamiltonians form a codimension $(2\nu - 2)$ subspace, since H_0 is arbitrary, $\dim(H_1) = \nu^2$, and the total number of free parameters at fixed H_0 is $F_t = F + 1 + \nu = \nu^2 - 2(\nu + 1)$. This is a remarkable result, since it shows that flat band Hamiltonians are only weakly fine-tuned, e.g., for $\nu = 3$, we find five free parameters when choosing the nine elements of H_1 for an arbitrary chosen H_0. Note that the above counting does not apply to the case $\nu = 2$ which was studied in Ref. [44] and amounts to two free parameters when choosing the four elements of H_1.

Equations (16) and (18) provide the complete solution to the problem of finding all the $d = 1$ nearest-neighbor Hamiltonians with one flat band and CLS of class $U = 2$. Figure 1 shows some examples of $U = 2$ and $\nu = 3$ Hamiltonians constructed using the above scheme.

For a bipartite network, the hopping matrix H_1 has a specific structure given by Eqs. (7) that simplifies Eqs. (15) to

$$S|\varphi_2\rangle = -A|\varphi_1\rangle, \tag{19}$$

$$S|\varphi_1\rangle = 0, \tag{20}$$

$$T|\varphi_1\rangle = -A|\varphi_2\rangle, \tag{21}$$

$$T|\varphi_2\rangle = 0, \tag{22}$$

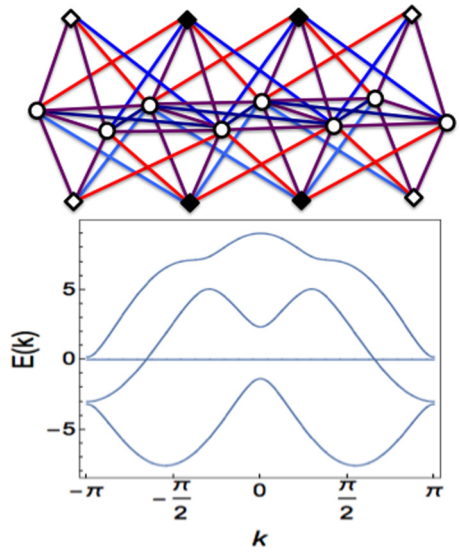

FIG. 2. Example of a bipartite flat band Hamiltonian with $U = 2$, $\nu = 4$. The sites of the CLS are indicated by the filled black squares. Links are colored differently for the convenience of visualisation of the chain. In this example, the chiral symmetry is broken on the minority sublattice, due to the presence of $B \neq 0, W \neq 0$ in Eq. (7). Nevertheless the chiral flat band is preserved. The details of this example are given in Appendix D 1.

and $E_{\rm FB} = 0$. The minority sublattice hopping matrices B, W dropped out as expected. The above equations are considerably simpler than the generic $U = 2$ Eqs. (15): the above system splits into two independent inverse eigenvalue problems for S and T. The details of the solution are presented in Appendix B 3, the final answer is

$$S = -\frac{A|\varphi_1\rangle\langle\varphi_2|Q_1}{\langle\varphi_2|Q_1|\varphi_2\rangle} + K_S Q_{12},$$
$$T = -\frac{A|\varphi_2\rangle\langle\varphi_1|Q_2}{\langle\varphi_1|Q_2|\varphi_1\rangle} + K_T Q_{12}, \tag{23}$$

where K_T and K_S are arbitrary matrices of size $(\nu - \mu) \times \mu$, respectively. The Q_{12} is a joint transverse projector on $|\varphi_{1,2}\rangle$. There are no restrictions on the entries of A, B, W, and $|\varphi_{1,2}\rangle$—they are all free parameters—at variance with the generic $U = 2$ flat band construction. Therefore the number of free parameters is $(\nu - \mu)(2\nu + \mu - 2) - 1$ (see Appendix B 3 for details). The above solution fails for $\langle\varphi_2|Q_1|\varphi_2\rangle = \langle\varphi_1|Q_2|\varphi_1\rangle \equiv 0$, therefore $|\varphi_2\rangle \propto |\varphi_1\rangle$, the CLS and the flat band are of class $U = 1$.

Figure 2 shows an example of a bipartite lattice with $\nu = 4$. There are two sites in the unit cell of each sublattice, and $B \neq 0$, $W \neq 0$. In this example, the parameters $\vec{\varphi}_2$, $\vec{\varphi}_2$, A, B, W are arbitrarily chosen, and $K_T = 0$, $K_S = 0$ (see details in the Appendix D 1).

B. $U \geqslant 3$

Let us consider larger U values. For simplicity, we use $U = 3$ in the examples. Fix the number of bands to ν, and choose some H_0, $E_{\rm FB}$, and $|\psi_1\rangle$. Then we have the following inverse eigenvalue problem with $U + 2$ equations (U for each CLS occupied unit cell, and two for the destructive interference conditions):

$$\begin{aligned} H_1|\psi_2\rangle &= (E_{\rm FB} - H_0)|\psi_1\rangle, \\ H_1^\dagger|\psi_1\rangle + H_1|\psi_3\rangle &= (E_{\rm FB} - H_0)|\psi_2\rangle, \\ H_1^\dagger|\psi_2\rangle &= (E_{\rm FB} - H_0)|\psi_3\rangle, \\ H_1|\psi_1\rangle &= 0, \\ H_1^\dagger|\psi_3\rangle &= 0. \end{aligned} \tag{24}$$

The set of constraints for the $\Psi_{\rm CLS}$ reads

$$\begin{aligned} \langle\psi_1|\psi_3\rangle &= 1, \\ \langle\psi_1|H_0|\psi_3\rangle &= E_{\rm FB}, \\ \langle\psi_1|E_{\rm FB} - H_0|\psi_2\rangle &= \langle\psi_2|E_{\rm FB} - H_0|\psi_3\rangle, \\ \langle\psi_1|E_{\rm FB} - H_0|\psi_1\rangle + \langle\psi_3|E_{\rm FB} - H_0|\psi_3\rangle & \\ = \langle\psi_2|E_{\rm FB} - H_0|\psi_2\rangle. & \end{aligned} \tag{25}$$

Again these identities are derived from Eqs. (24) by multiplying them with $\langle\psi_1|$ and $\langle\psi_U|$ and rearranging terms, in order to eliminate H_1. Notice that the set of compatibility constraints for $\Psi_{\rm CLS}$ amounts to $U + 1$ equations. Note also that in precisely two of those $U + 1$ equations, with $\langle\psi_1|$ given, amount to 2 linear, and $U - 1$ nonlinear equations for the remaining CLS amplitudes. It is not possible to solve the nonlinear equations analytically in general, but we present in Appendix C 2 a numerical algorithm that allows to resolve these constraints and enumerate all the solutions, if existing, for the case $U = 3$.

Instead of using the *Ansatz* (17) for H_1, we take a more suitable approach to generate flat band Hamiltonians (i.e., matrices H_1) for $U \geqslant 3$. With a given $\Psi_{\rm CLS}$, which satisfies the constraints (25), the set of equations (24) is a linear system with respect to H_1:

$$T\, h_1 = \Lambda. \tag{26}$$

Here, h_1 is a ν^2-dimensional vector resulting from the vectorization of the matrix H_1. T is a rectangular $\nu(U + 2) \times \nu^2$ matrix whose elements are composed by the elements of CLS, such that the product $T\, h_1$ is the left-hand side of Eqs. (24). Λ is a $\nu(U + 2)$ vector originating from the right-hand side of Eqs. (24):

$$\Lambda = (E_{\rm FB} - H_0) \begin{pmatrix} \vec{\psi}_1 \\ \vec{\psi}_2 \\ \cdots \\ \vec{\psi}_U \\ \vec{0} \\ \vec{0} \end{pmatrix}. \tag{27}$$

The zero vector components $\vec{0}$ result from the destructive interference. The linear system (26) can be then solved, e.g., using a least squares solver. Figure 3 shows some examples

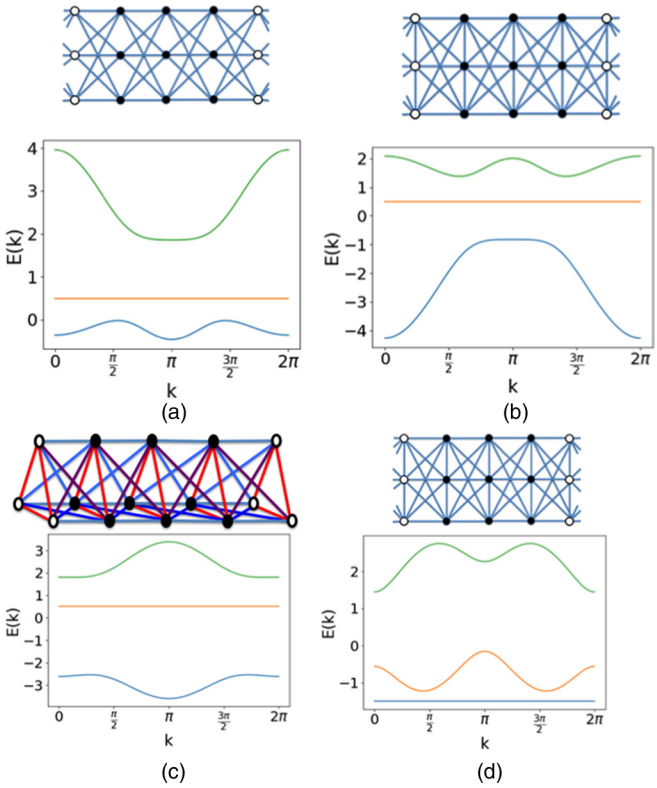

FIG. 3. Examples of Hamiltonians with a CLS of class $U = 3$. The sites occupied by a CLS are indicated by black filled circles. (a) Diagonal choice for H_0. (b) Chain like structure for H_0. (c) Generic choice for H_0. (d) E_{FB} is chosen negative enough to become the groundstate. Details of these examples are presented in Appendix D 2.

of $U = 3$ flat bands, which we generated by resolving the constraints (25) and solving Eq. (26).

C. Network constraints

For practical purposes, the flat band fine-tuning of a Hamiltonian network can involve additional network constraints, e.g. the strict vanishing of certain hopping terms between specific sites of the network [54]. This typically happens when arranging network sites in a plane. Let us consider the typical problem of finding a nearest-neighbor flat band Hamiltonian with specific network constraints. These network constraints dictate the locations of zero entries in H_0 and H_1. They can be incorporated into the matrix T of Eq. (26) as a mask M: $T \to TM$ that enforces zero entries in H_1 in the right positions. The solution of the resulting system is then searched for similar to the nonconstrained case.

Especially when H_0 and H_1 are sparse, e.g., the number of variables in H_1 is equal to or greater then the number of equations, it is possible to solve (8)–(12) analytically (see Appendix E). Figure 4 shows examples of networks with flat bands generated for a $d = 1$ kagome chain and chains with hoppings allowed only inside network plaquettes.

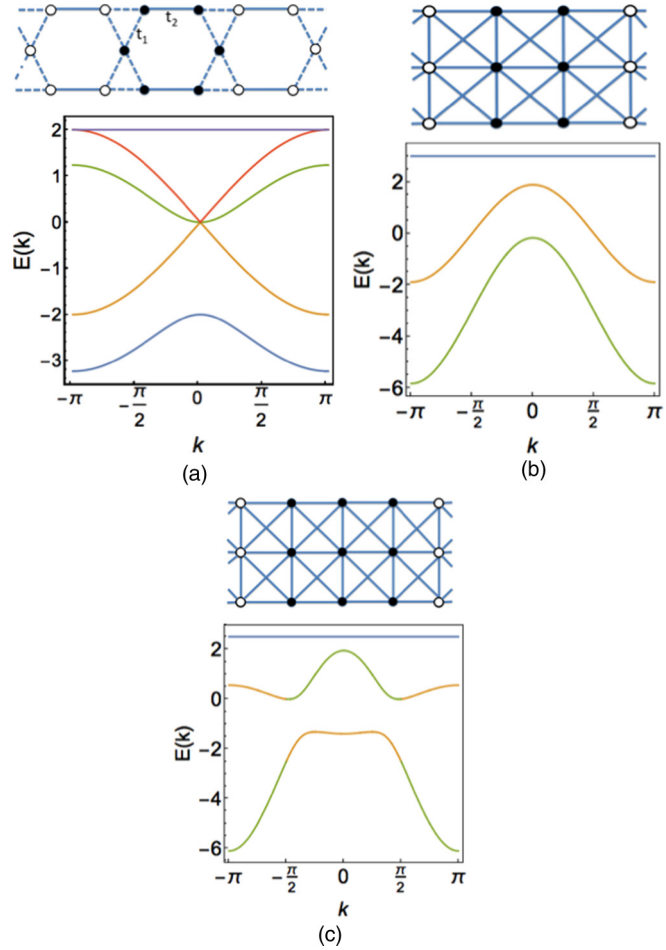

FIG. 4. Examples of flat band Hamiltonians constructed on specific networks. The sites occupied by a CLS are marked by black filled circles. (a) 1d kagome with $\nu = 5$ and $U = 2$ compact localized states. The crossing of three bands indicates that the Hamiltonian can be detangled into two independent sub-Hamiltonians. (b) and (c) Examples of Hamiltonians with $\nu = 3$, $U = 2$ and $U = 3$ CLS, respectively. The details of all these Hamiltonians are provided in Appendix E.

V. CONCLUSIONS

We presented a systematic construction of one-dimensional Hamiltonians with ν bands including one flat band for an arbitrary size $U \leqslant \nu$ of compact localized states and illustrated the method with several examples. The task of finding flat band Hamiltonians is reduced to solving a specific inverse eigenvalue problems subject to certain nonlinear constraints. The flat band energy enters as a parameter and can be tuned. For the $U = 2$ case, we derive analytical solutions to the inverse eigenvalue problem supplemented with a numerical algorithm to resolve for the constraints. For $U \geqslant 3$, analytical solutions are not accessible, yet numerical algorithms are applied to generate flat band Hamiltonians. We illustrate the method by generating several $U = 3$ flat band Hamiltonians. The same construction allows to incorporate various network geometry constraints into the search algorithm. Our results show that flat band Hamiltonians, while being the result of a fine-tuning in the space of all tight binding Hamiltonian networks, allow for

a surprisingly large number of free parameters which change the network, but leave the flatness of the flat band untouched.

Open questions include the extension of the present formalism to the case of multiple flat bands and/or higher dimensions. The present algorithm can be extended naturally to higher dimensions and will generalize the approach of Nishino *et al.* [10,42]. The extension to $d = 2,\ 3$ would require more intercell hopping matrices H_a describing hopping in different dimensions—H_x, H_y in the simplest case of the square lattice geometry—beyond just H_1. Also the simple classification in terms of the CLS size U has to be extended: one has to specify the shape of the compact localised state. Equations (1) regarded as an inverse eigenvalue problem would now couple different H_a. These equations can be decoupled with respect to H_a by introducing additional variables, and reduced to inverse eigenvalue problems for individual hopping matrices H_a, similar to the ones that we were solving here for $d = 1$.

Another interesting interesting avenue for future research is the case of non-Hermitian Hamiltonians allowing for gain and loss terms in the Hamiltonian (2). Recently a number of works [55,56] analyzed flat bands in such systems or considered the fate of flat bands in the presence of non-Hermitian perturbations [50,57] and finding interesting results. Finally, non-Hermitian Hamiltonians have a larger parameter space suggesting richer classification as compared to the Hermitian case. We expect therefore that a systematic construction and identification of flat bands in this context might lead to new interesting results.

ACKNOWLEDGMENT

This work was supported by the Institute for Basic Science in Korea (IBS-R024-D1).

APPENDIX A: REDUCTION OF CLS OF CLASS U INTO $U-1$, WHEN $\vec{\psi}_1 \perp \vec{\psi}_U$.

Suppose we have a CLS of class U, that we write as $\vec{\psi}_{cls} = (\vec{\psi}_1, \vec{\psi}_2, \ldots, \vec{\psi}_U)^T$, and $\vec{\psi}_1 \perp \vec{\psi}_U$. Then we can apply a unitary transformation R on the CLS, such that $\tilde{\vec{\psi}}_i = R\vec{\psi}_i,\ i = 1, \ldots, U$. and

$$\tilde{\vec{\psi}}_1 = \begin{bmatrix} 1 \\ 0 \\ \vdots \\ 0 \end{bmatrix}, \quad \tilde{\vec{\psi}}_2 = \begin{bmatrix} \psi_2^1 \\ \psi_2^2 \\ \vdots \\ \psi_2^\nu \end{bmatrix}, \ldots, \quad \tilde{\vec{\psi}}_U = \begin{bmatrix} 0 \\ \psi_U^2 \\ \vdots \\ \psi_U^\nu \end{bmatrix}, \tag{A1}$$

where ν is number of sites per unit cell. Due to unitary of transformation R, the eigenvalue problem (8)–(12) does not change. Next we redefine the unit cell in the following way:

$$\tilde{\vec{\psi}}_1 = \begin{bmatrix} 1 \\ \psi_2^2 \\ \vdots \\ \psi_2^\nu \end{bmatrix}, \ \tilde{\vec{\psi}}_2 = \begin{bmatrix} \psi_2^1 \\ \psi_3^2 \\ \vdots \\ \psi_3^\nu \end{bmatrix}, \ldots, \ \tilde{\vec{\psi}}_{U-1} = \begin{bmatrix} \psi_{U-1}^1 \\ \psi_U^2 \\ \vdots \\ \psi_U^\nu \end{bmatrix},$$

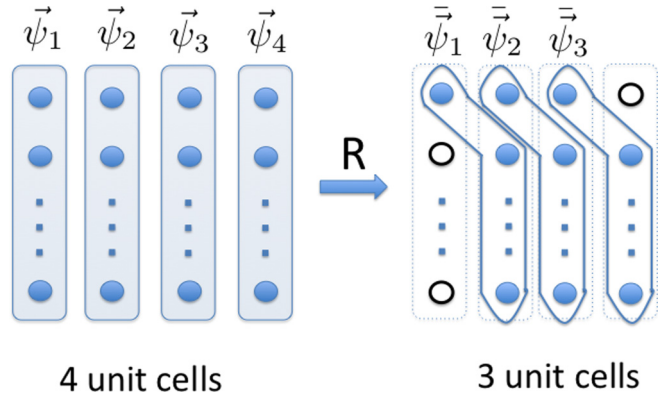

FIG. 5. A schematics showing how a CLS of class $U = 4$ reduces to $U = 3$, when $\vec{\psi}_1 \perp \vec{\psi}_4$. Each elongated box stands for one unit cell. Filled circles: nonzero wave function components. Open circles: zero wave function components.

and $\bar{\vec{\psi}}_U = 0$. Therefore, after the unitary transformation R and redefinition of the unit cell, the class of the CLS reduces to $U - 1$. The schematics of this procedure is shown in Fig. 5.

APPENDIX B: INVERSE EIGENVALUE PROBLEM: A TOY EXAMPLE AND THE SOLUTION OF THE $U = 2$ CLS

This Appendix explains the solution of the inverse eigenvalue problems (15). As discussed in main text, 1D flat band lattices with CLS class U satisfy

$$\begin{aligned} H_1\vec{\psi}_2 &= (E_{\rm FB} - H_0)\vec{\psi}_1, \\ H_1^\dagger\vec{\psi}_{l-1} + H_1\vec{\psi}_{l+1} &= (E_{\rm FB} - H_0)\vec{\psi}_l, \quad l = 2, \ldots, U-1, \\ H_1^\dagger\vec{\psi}_{U-1} &= (E_{\rm FB} - H_0)\vec{\psi}_U, \\ H_1\vec{\psi}_1 &= 0, \\ H_1^\dagger\vec{\psi}_U &= 0. \end{aligned} \tag{B1}$$

Assuming that $E_{\rm FB}, H_0, \vec{\psi}_{l=1,\ldots,U}$ are given, the equations (B1) constitute an inverse eigenvalue problem for a block-tridiagonal matrix, where diagonal blocks are H_0 and off diagonal ones are H_1.

1. Toy example

As a warmup, we solve a toy inverse eigenvalue problem: reconstruct $\nu \times \nu$ matrix T given its action $|y\rangle$ on some vector $|x\rangle$

$$T\,|x\rangle = |y\rangle. \tag{B2}$$

The solution is not unique: generic solution can be represented as $T = T_* + \delta T$, where T_* is any particular solution of Eq. (B2) and $\delta T\,|x\rangle = 0$. One possible particular solution is easily found to be

$$T_* = \frac{|y\rangle\langle x|}{\langle x||x\rangle}, \quad \delta T = Q_x K, \tag{B3}$$

where Q_x is a transverse projector on x. This construction generalizes straightforwardly to the case of many vectors (we

assume here implicitly that the equations are consistent):

$$T|x_k\rangle = |y_k\rangle, \quad k = 1, \ldots, m. \tag{B4}$$

The generic solution to this problem is given by

$$T_* = \sum_{ij} A_{ij}|y_i\rangle\langle x_j|, \quad A^{-1}_{ij} = \langle x_i||x_j\rangle, \tag{B5}$$

$$\delta T = Q\,K, \tag{B6}$$

where Q is the orthogonal projector on the subspace spanned by $\{x_k\}$ and K is an arbitrary $\nu \times \nu$ matrix. For later convenience, we refer to T_* as *particular solution* and δT as *free part*.

2. $U = 2$ case

In this case, Eq. (B1) reads

$$\begin{aligned} H_1|\psi_2\rangle &= (E_{\rm FB} - H_0)|\psi_1\rangle, \\ H_1^\dagger|\psi_1\rangle &= (E_{\rm FB} - H_0)|\psi_2\rangle, \\ H_1|\psi_1\rangle &= 0, \\ H_1^\dagger|\psi_2\rangle &= 0. \end{aligned} \tag{B7}$$

We know H_0, $|\psi_1\rangle$, $|\psi_2\rangle$ and $E_{\rm FB} = \langle\psi_1|H_0|\psi_2\rangle$, and we need to determine H_1. As discussed above for the toy case, the generic solution to this problem can be decomposed into a particular solution and a free part. The last two equations in the above set are satisfied by the following *Ansatz*:

$$H_1 = Q_2 M Q_1, \quad Q_i = \mathbb{I} - \frac{|\psi_i\rangle\langle\psi_i|}{\langle\psi_i|\psi_i\rangle}. \tag{B8}$$

Plugging this *Ansatz* back into the system, we find

$$\begin{aligned} Q_2\,M\,Q_1|\psi_2\rangle &= (E_{\rm FB} - H_0)|\psi_1\rangle, \\ \langle\psi_1|Q_2\,M\,Q_1 &= \langle\psi_2|(E_{\rm FB} - H_0). \end{aligned} \tag{B9}$$

Note the identity

$$\langle\psi_1|H_1|\psi_2\rangle = \langle\psi_1|E_{\rm FB} - H_0|\psi_1\rangle = \langle\psi_2|E_{\rm FB} - H_0|\psi_2\rangle, \tag{B10}$$

that follows straightforwardly from the first two equations of (B7). Defining the projectors

$$\begin{aligned} R_{12} &= \mathbb{I} - \frac{Q_1|\psi_2\rangle\langle\psi_2|Q_1}{\langle\psi_1|Q_1|\psi_1\rangle}, \\ R_{21} &= \mathbb{I} - \frac{Q_2|\psi_1\rangle\langle\psi_1|Q_2}{\langle\psi_1|Q_2|\psi_1\rangle}, \end{aligned} \tag{B11}$$

we can write

$$M = T + R_{21}\,K\,R_{12}, \tag{B12}$$

where T is a particular solution of Eq. (B9). The second term, where K is an arbitrary $\nu \times \nu$ matrix, satisfies Eqs. (B9) by construction and is the free part of the solution. Therefore we only need to find a particular solution to the system to get the generic solution. This is achieved by the same *Ansatz* $T = |x\rangle\langle y|$ as in the toy case discussed above. The *Ansatz* yields the following equations:

$$Q_2\,T\,Q_1|\psi_2\rangle = \langle y|Q_1|\psi_2\rangle Q_2|x\rangle = (E_{\rm FB} - H_0)|\psi_1\rangle, \tag{B13}$$

$$\langle\psi_1|Q_2\,T\,Q_1 = \langle\psi_1|Q_2|x\rangle\langle y|Q_1 = \langle\psi_2|(E_{\rm FB} - H_0). \tag{B14}$$

From these, the vectors x and y are fixed (up to unimportant normalization):

$$\begin{aligned} \langle y|Q_1 &= \frac{1}{\langle\psi_1|Q_2|x\rangle}\langle\psi_2|(E_{\rm FB} - H_0), \\ Q_2|x\rangle &= \frac{1}{\langle y|Q_1|\psi_2\rangle}(E_{\rm FB} - H_0)|\psi_1\rangle \\ &= \frac{\langle\psi_1|Q_2|x\rangle}{\langle\psi_2|E_{\rm FB} - H_0|\psi_2\rangle}(E_{\rm FB} - H_0)|\psi_1\rangle \\ &= \frac{\langle\psi_1|Q_2|x\rangle}{\langle\psi_1|E_{\rm FB} - H_0|\psi_1\rangle}(E_{\rm FB} - H_0)|\psi_1\rangle. \end{aligned}$$

We used the condition (B10) to replace the denominator in the fourth line. Also note that the expression for y from the first line was used to simplify the second line, and eliminate y. The particular solution is then

$$Q_2 T Q_1 = \frac{(E_{\rm FB} - H_0)|\psi_1\rangle\langle\psi_2|(E_{\rm FB} - H_0)}{\langle\psi_1|E_{\rm FB} - H_0|\psi_1\rangle}. \tag{B15}$$

Thanks to (B10) it is symmetric with respect to $|\psi_1\rangle, |\psi_2\rangle$. This and the above mentioned free part $Q_{21}KQ_{12}$ give the full family of solutions (18):

$$H_1 = \frac{(E_{\rm FB} - H_0)|\psi_1\rangle\langle\psi_2|(E_{\rm FB} - H_0)}{\langle\psi_1|E_{\rm FB} - H_0|\psi_1\rangle} + Q_2 R_{21} K R_{12} Q_1.$$

This expression is further simplified by noticing that $R_{12}Q_1$ and Q_2R_{21} are the same projector on the subspace spanned by $|\psi_1\rangle, |\psi_2\rangle$, that we denote Q_{12}: $(R_{12}Q_1)^2 = R_{12}Q_1$, idem for Q_2R_{21} and both vanish when acting on $|\psi_{1,2}\rangle$ as can be straightforwardly verified. We can therefore replace these combinations by Q_{12}:

$$H_1 = \frac{(E_{\rm FB} - H_0)|\psi_1\rangle\langle\psi_2|(E_{\rm FB} - H_0)}{\langle\psi_1|E_{\rm FB} - H_0|\psi_1\rangle} + Q_{12} K Q_{12}. \tag{B16}$$

This solution is supplemented by the following nonlinear constraints:

$$\begin{aligned} \langle\psi_2|\psi_1\rangle &= 1, \\ \langle\psi_2|H_0|\psi_1\rangle &= E_{\rm FB}, \\ \langle\psi_1|E_{\rm FB} - H_0|\psi_1\rangle &= \langle\psi_2|E_{\rm FB} - H_0|\psi_2\rangle, \end{aligned} \tag{B17}$$

that are obtained by eliminating H_1 from Eq. (B7) using "destructive interference conditions," i.e., last two equations in Eq. (B7).

In case the denominator in Eq. (B16) is zero, the single projector *Ansatz* fails, and two projector *Ansatz* has to be used:

$$\begin{aligned} H_1 = &\frac{(E_{\rm FB} - H_0)|\psi_1\rangle\langle\psi_2|Q_1}{\langle\psi_2|Q_1|\psi_2\rangle} \\ &+ \frac{Q_2|\psi_1\rangle\langle\psi_2|(E_{\rm FB} - H_0)}{\langle\psi_1|Q_2|\psi_1\rangle} + Q_{12} K Q_{12}, \end{aligned} \tag{B18}$$

as can be verified by a direct substitution. In this special solution, the denominators only vanish when $\Psi_1 \propto \Psi_2$, i.e., in $U = 1$ case.

3. Bipartite lattices and chiral symmetry

In this section, we solve the inverse eigenvalue problem for $U = 2$ for the special case of bipartite lattices. We consider a bipartite lattice with ν sites per unit cell that split into majority and minority sublattices with μ and $\nu - \mu$ sites, respectively. Since the lattice is bipartite, the sites on one sublattice only have neighbours belonging to the other sublattice. This enforces the following structure on the hopping matrices and the wave functions of the CLS [see Eqs. (7)]:

$$H_0 = \begin{pmatrix} 0 & A^\dagger \\ A & B \end{pmatrix}, \quad H_1 = \begin{pmatrix} 0 & T^\dagger \\ S & W \end{pmatrix},$$
$$\vec{\psi}_1 = \begin{pmatrix} \varphi_1 \\ 0 \end{pmatrix}, \quad \vec{\psi}_2 = \begin{pmatrix} \varphi_2 \\ 0 \end{pmatrix}. \tag{B19}$$

Here, $\varphi_{1,2}$ are μ component vectors describing the wave amplitudes of the majority sublattice sites. A, S, T are $(\nu - \mu) \times \mu$ matrices, while B, W are $(\nu - \mu) \times (\nu - \mu)$ matrices. B and W formally break the bipartiteness of the lattice, but do not affect the $E_{\mathrm{FB}} = 0$ flat band(s). This special structure simplifies Eqs. (B7):

$$S|\varphi_2\rangle = -A|\varphi_1\rangle, \tag{B20}$$
$$T|\varphi_1\rangle = -A|\varphi_2\rangle, \tag{B21}$$
$$S|\varphi_1\rangle = 0, \tag{B22}$$
$$T|\varphi_2\rangle = 0. \tag{B23}$$

These equations need to be resolved with respect to S and T. The last two equations are satisfied by the *Ansätze* $S = S'Q_1$, $T = T'Q_2$, where Q_i is a transverse projector on φ_i. The remaining two equations are identical to the toy problem that we discussed above(see Appendix B 1) and their solution is precisely Eqs. (23):

$$S = -\frac{A|\varphi_1\rangle\langle\varphi_2|Q_1}{\langle\varphi_2|Q_1|\varphi_2\rangle} + K_S Q_{12}, \tag{B24}$$
$$T = -\frac{A|\varphi_2\rangle\langle\varphi_1|Q_2}{\langle\varphi_1|Q_2|\varphi_1\rangle} + K_T Q_{12}, \tag{B25}$$

where Q_{12} is a joint transverse projector on $|\varphi_{1,2}\rangle$.

Now let's count the number of free parameters. $|\varphi_1\rangle$ and $|\varphi_2\rangle$ all are free parameters each contains μ free parameters. A contains $(\nu - \mu)\mu$ free variables. B, W each contains $(\nu - \mu)^2$ free parameters. $K_S Q_{12}$ and $Q_{21}K_T$ are $(\nu - \mu) \times \mu$ and $\mu \times (\nu - \mu)$ matrices, and, because of the transverse projectors, they contain $(\nu - \mu)(\mu - 2)$ and $\mu(\nu - \mu - 2)$ free parameters respectively. Therefore total number of free parameters in the solution (B24) contains $2\mu - 1 + (\nu - \mu)\mu + (\nu - \mu)(\mu - 2) + \mu(\nu - \mu - 2) + 2(\nu - \mu)^2 = (\nu - \mu)(2\nu + \mu - 2) - 1$ free parameters. The extra -1 corresponds to the overall normalisation of the CLS, that is not fixed.

APPENDIX C: RESOLVING THE NONLINEAR CONSTRAINTS

Let us discuss how one can efficiently resolve the set of nonlinear constraints, that appear in the inverse eigenvalue problem, for example (B17). Since these are a nonlinear system of equations, one can always try a numerical solver. However our experience was not particularly successful: the solver was not converging and finding no solution more often than not. Instead it is possible to design an numerical algorithm that eliminates constraints one by one and either founds and enumerates all the solutions, or proves that there are none.

1. $U = 2$ case

The nonlinear equations that we need to solve are

$$\langle\psi_1|\psi_2\rangle = 1, \tag{C1}$$
$$\langle\psi_1|H_0|\psi_2\rangle = E_{\mathrm{FB}}, \tag{C2}$$
$$\langle\psi_1|E_{\mathrm{FB}} - H_0|\psi_1\rangle = \langle\psi_1|E_{\mathrm{FB}} - H_0|\psi_1\rangle. \tag{C3}$$

We assume that E_{FB}, H_0, and ψ_1 (or ψ_2) are given input parameters.

Then we need to solve the above equations for ψ_2. The first two equations (C1) and (C2) are linear and are easily satisfied with the following expansion for ψ_2, by the choice of the basis vectors e_1 and e_2:

$$|\psi_2\rangle = \sum_{k=1}^{\nu} x_k |e_k\rangle, \tag{C4}$$
$$|e_1\rangle = \frac{1}{\sqrt{\langle\psi_1||\psi_1\rangle}}|\psi_1\rangle, \tag{C5}$$
$$|e_2\rangle = \frac{1}{\sqrt{\langle\psi_1|H_0Q_1H_0|\psi_1\rangle}} Q_1 H_0|\psi_1\rangle, \tag{C6}$$
$$\langle e_l||e_m\rangle = \delta_{lm}, \quad l, m = 1, 2, \ldots \nu. \tag{C7}$$

Here, Q_1 is a transverse projector on $|\psi_1\rangle$. With this choice of the basis vectors the equations (C1) and (C2) imply:

$$x_1 = \frac{1}{\sqrt{\langle\psi_1||\psi_1\rangle}},$$
$$x_2 = \frac{1}{\sqrt{\langle\psi_1|H_0Q_1H_0|\psi_1\rangle}}\left[E_{\mathrm{FB}} - \frac{\langle\psi_1|H_0|\psi_1\rangle}{\langle\psi_1||\psi_1\rangle}\right].$$

The remaining basis vectors are fixed by requiring their orthonormality, for example, by using Gram-Schmidt orthogonalization. Next we plug the expansion (C4) into Eq. (C3) and separate out the terms with e_1 and e_2:

$$\begin{aligned}\langle\psi_1|E_{\mathrm{FB}} - H_0|\psi_1\rangle &= \sum_{ij=1}^{\nu} x_i^* x_j \langle e_i|E_{\mathrm{FB}} - H_0|e_j\rangle \\ &= \sum_{ij=1}^{2} x_i^* x_j \langle e_i|E_{\mathrm{FB}} - H_0|e_j\rangle \\ &\quad + \sum_{i=1}^{2}\sum_{j=3}^{\nu}[x_i^* x_j \langle e_i|E_{\mathrm{FB}} - H_0|e_j\rangle \\ &\quad + x_j^* x_i \langle e_j|E_{\mathrm{FB}} - H_0|e_i\rangle] \\ &\quad + \sum_{ij=3}^{\nu} x_i^* x_j \langle e_i|E_{\mathrm{FB}} - H_0|e_j\rangle.\end{aligned}$$

This expression can be rewritten as follows:

$$\sum_{ij=1}^{\nu-2} y_i^* M_{ij} y_j + \sum_{i=1}^{\nu-2} [u_i^* y_i + u_i y_i^*] = w, \tag{C8}$$

$$M_{ij} = \langle e_{i+2}|E_{\rm FB} - H_0|e_{j+2}\rangle, \tag{C9}$$

$$u_i = \sum_{j=1}^{2} x_j \langle e_{i+2}|E_{\rm FB} - H_0|e_j\rangle, \tag{C10}$$

$$w = \sum_{ij=1}^{2} x_i^* x_j \langle e_i|E_{\rm FB} - H_0|e_j\rangle - \langle \psi_1|E_{\rm FB} - H_0|\psi_1\rangle, \tag{C11}$$

where $y_i = x_{i+2}$. The equations on y_i are further simplified by the shift: $z_i = y_i + M_{ij}^{-1} u_j$, that eliminates the linear term. This gives the following equation on a quadratic form:

$$\sum_{ij=1}^{\nu-2} z_i^* M_{ij} z_j = w + \sum_{ij=1}^{\nu-2} u_i^* M_{ij} u_j. \tag{C12}$$

Notice that the RHS of the above equation is real. The matrix M is Hermitian, and can be diagonalized: $M_{ij} = \sum_\alpha E_\alpha |r_\alpha\rangle\langle r_\alpha|$. The above equation is solved with the help of this spectral decomposition:

$$\sum_{\alpha=1}^{\nu-2} E_\alpha |t_\alpha|^2 = \tilde{w}, \tag{C13}$$

$$\tilde{w} = w + \sum_{\alpha=1}^{\nu-2} E_\alpha |s_\alpha|^2, \tag{C14}$$

$$t_\alpha = \langle r_\alpha||z_\alpha\rangle, \quad s_\alpha = \langle r_\alpha||u\rangle. \tag{C15}$$

The presence or absence of solution is decided by the mutual signs of $\tilde{w}$ and E_α: if $\tilde{w} > 0$ and $E_\alpha < 0$ $\forall\alpha$, then there is no solution. If one $E_\alpha > 0$, there is a single solution, for two and more $E_\alpha > 0$ there is a multiparametric family of solutions. Knowing t_α, it is straightforward to reconstruct the original $\vec{\psi}_2$.

In the above M, was assumed nonsingular. If it is singular, than M_{ij}^{-1} is the Moore-Pensrose pseudoinverse [58] and we have $y_i = z_i + g_i - M_{ij}^{-1} u_j$ where $g \in \ker M$. For g_i the quadratic terms in (C8) vanish (by definition of g_i) and the g_i only enter linearly the equation, while z_i can be treated as in the nonsingular case (for convenience we assume that the first k eigenvalues of M are zero):

$$\sum_{\alpha=k+1}^{\nu-2} E_\alpha t_\alpha^2 = \tilde{w} - \sum_{\alpha=1}^{k} [\langle u||r_\alpha\rangle + \langle r_\alpha||u\rangle]. \tag{C16}$$

The presence of zero modes renormalizes $\tilde{w}$.

The more refined version of the counting relies on the above solution, and the counting of the E_α with the "right" sign. It tells us that for $\nu = 2$ and 3, there is a single solution for fixed $\vec{\psi}_1$, $E_{\rm FB}$, H_0. For larger ν, there could be a single solution or multiparametric families of solutions, from 0 to $\nu - 3$.

2. $U = 3$ case

In this case, the nonlinear constraints read, Eq. (25),

$$\begin{aligned}
\langle \psi_1|\psi_3\rangle &= 1,\\
\langle \psi_1|H_0|\psi_3\rangle &= E_{\rm FB},\\
\langle \psi_1|E_{\rm FB} - H_0|\psi_2\rangle &= \langle \psi_2|E_{\rm FB} - H_0|\psi_3\rangle,\\
\langle \psi_3|E_{\rm FB} - H_0|\psi_3\rangle &= \langle \psi_2|E_{\rm FB} - H_0|\psi_2\rangle\\
&\quad - \langle \psi_1|E_{\rm FB} - H_0|\psi_1\rangle.
\end{aligned} \tag{C17}$$

The resolution of this set of constraint is very similar to the $U = 2$ case, therefore we only outline the main steps. We search to resolve the above equations with respect to Ψ_3, taking Ψ_1, Ψ_2 as inputs. The first three equations are linear, and we solve them by expanding Ψ_3 over a suitable orthonormal basis:

$$\begin{aligned}
|\psi_3\rangle &= \sum_k x_k |e_k\rangle,\\
|e_1\rangle &= \frac{1}{\sqrt{\langle \psi_1||\psi_1\rangle}}|\psi_1\rangle,\\
|e_2\rangle &= \frac{1}{\sqrt{\langle \psi_1|H_0 Q_1 H_0|\psi_1\rangle}} Q_1 H_0|\psi_1\rangle,\\
|e_3\rangle &= \frac{Q_*(E_{\rm FB} - H_0)|\psi_2\rangle}{\sqrt{\langle \psi_2|(E_{\rm FB} - H_0) Q_*(E_{\rm FB} - H_0)|\psi_2\rangle}},\\
&\vdots\\
\langle e_l||e_m\rangle &= \delta_{l,m}, \quad l, m = 1, 2, \ldots, \nu,\\
Q_1 &= \mathbb{I} - \frac{|\psi_1\rangle\langle\psi_1|}{\langle \psi_1||\psi_1\rangle},
\end{aligned}$$

and Q_* is a joint transverse projector on $|\psi_1\rangle$ and $Q_1 H_0|\psi_1\rangle$. Then x_1 and x_2 are the same as in the $U = 2$ case, x_3 is directly expressed through the third equation in Eqs. (C17). The last, fourth equation in (C17) is solved in the same way as that in the $U = 2$ case: it is reduced to solving a quadratic form.

APPENDIX D: EXAMPLES FOR FB GENERATORS

In this section, we present the details of the example flat band Hamiltonians generated using the algorithm discussed in the main text. In all of these examples we pick some H_0, $E_{\rm FB}$ and part of the ψ_l as an input. Next following the algorithm outlined in Appendix C we construct a set of $\{\psi_l\}$ consistent with the CLS structure. Then we find the hopping matrix H_1 using the algorithm from Sec. III B (detailed in Appendix B). For simplicity we drop the free part K in all the examples below.

1. $\nu = 3, U = 2$ case

Example shown in Fig. 1(a). We start with a three band case $\nu = 3$, and no additional constraints on the form of H_1. We assume canonical (diagonal) form of H_0 and choose $\vec{\psi}_1$

$$H_0 = \begin{bmatrix} 0 & 0 & 0\\ 0 & 1 & 0\\ 0 & 0 & 2 \end{bmatrix}, \quad \vec{\psi}_1 = (1, -1, 1), \tag{D1}$$

Using the FB algorithm, we find the particular solution:

$$E_{\mathrm{FB}} = 0.5, \quad \vec{\psi}_2 = (1.5,\ 1.5,\ 1), \tag{D2}$$

$$H_1 = \begin{bmatrix} -0.25 & 0.25 & 0.5 \\ -0.25 & 0.25 & 0.5 \\ 0.75 & -0.75 & -1.5 \end{bmatrix}, \tag{D3}$$

Example shown in Fig. 1(b). Taking nondiagonal H_0 and $\vec{\psi}_1$ as

$$H_0 = \begin{bmatrix} 0 & 1 & 0 \\ 1 & 0 & 1 \\ 0 & 1 & 0 \end{bmatrix}, \quad \vec{\psi}_1 = (1, -1, 1), \tag{D4}$$

we construct the following FB Hamiltonian:

$$H_1 = \begin{bmatrix} 0.19926929 & -0.47727273 & -0.67654202 \\ -0.33211549 & 0.79545455 & 1.12757003 \\ 0.19926929 & -0.47727273 & -0.67654202 \end{bmatrix}, \tag{D5}$$

$$\vec{\psi}_2 = (4.46130814,\ 1.5,\ -1.96130814),\ E_{\mathrm{FB}} = 0.5 \tag{D6}$$

Example shown in Fig. 1(c). Taking all the sites in the unit cell connected to each other and the same $\vec{\psi}_1$, E_{FB} as in the above example

$$H_0 = \begin{bmatrix} 0 & 1 & 1 \\ 1 & 0 & 1 \\ 1 & 1 & 0 \end{bmatrix}, \quad \vec{\psi}_1 = (1, -1, 1), \tag{D7}$$

we land at the following Hamiltonian:

$$H_1 = \begin{bmatrix} 0.18163216 & -0.16071429 & -0.34234644 \\ -0.90816078 & 0.80357143 & 1.71173221 \\ 0.18163216 & -0.16071429 & -0.34234644 \end{bmatrix}, \tag{D8}$$

$$\vec{\psi}_2 = (1.84761673,\ 0.25,\ -0.59761673),\ E_{\mathrm{FB}} = 0.5. \tag{D9}$$

Bipartite lattice $U = 2$, Fig. 2. We consider the $\nu = 4$, $\mu = 2$ case and pick the following input variables:

$$A = \frac{1}{4}\begin{pmatrix} \sqrt{3} & 1 \\ 3 & \sqrt{3} \end{pmatrix}, \quad B = \begin{pmatrix} 1 & -2 \\ -2 & 1 \end{pmatrix},$$
$$\vec{\varphi}_1 = \frac{1}{\sqrt{2}}(1, 1), \quad \vec{\varphi}_2 = \frac{1}{2}(1, \sqrt{3}),$$
$$W = \begin{pmatrix} 2 & -1 \\ -1 & 2 \end{pmatrix}.$$

Solving Eqs. (23) and (B24) yields the following solution:

$$S = \frac{(\sqrt{3}+2)\begin{pmatrix} -1 & 1 \\ -\sqrt{3} & \sqrt{3} \end{pmatrix}}{2\sqrt{2}},$$
$$T = \frac{(\sqrt{3}+1)\begin{pmatrix} 3 & 3\sqrt{3} \\ -\sqrt{3} & -3 \end{pmatrix}}{4\sqrt{2}}.$$

The corresponding hopping matrices H_0 and H_1 read

$$H_0 = \begin{pmatrix} 0 & 0 & \frac{\sqrt{3}}{4} & \frac{3}{4} \\ 0 & 0 & \frac{1}{4} & \frac{\sqrt{3}}{4} \\ \frac{\sqrt{3}}{4} & \frac{1}{4} & 1 & -2 \\ \frac{3}{4} & \frac{\sqrt{3}}{4} & -2 & 1 \end{pmatrix},$$
$$H_1 = \begin{pmatrix} 0 & T \\ S & W \end{pmatrix},$$
$$\vec{\psi}_1 = \left(\frac{1}{\sqrt{2}}, \frac{1}{\sqrt{2}}, 0, 0\right),$$
$$\vec{\psi}_2 = \left(\frac{1}{2}, \frac{\sqrt{3}}{2}, 0, 0\right).$$

2. $\nu = 3, U = 3$ case

Example shown in Fig. 3(a). We pick H_0 in canonical form and choose $\vec{\psi}_1$ as follows:

$$H_0 = \begin{bmatrix} 0 & 0 & 0 \\ 0 & 1 & 0 \\ 0 & 0 & 2 \end{bmatrix}, \quad \vec{\psi}_1 = (1, -1, 1).$$

Solving the nonlinear constraints (25) and (C17), we get $\vec{\psi}_2, \vec{\psi}_3$. Then solving the equation (26), which is equivalent to equations (8) and (12), we get

$$H_1 = \begin{bmatrix} -0.06548573 & -0.27210532 & -0.2066196 \\ -0.15130619 & -0.28682832 & -0.13552213 \\ -0.14682469 & 0.75742396 & 0.90424865 \end{bmatrix},$$
$$\vec{\psi}_2 = (-0.05144152, -1.53640189, -0.38025523),$$
$$\vec{\psi}_3 = (0.58333333, -0.33333333, 0.08333333),$$
$$E_{\mathrm{FB}} = 0.5.$$

Example shown in Fig. 3(b). We choose H_0 and $\vec{\psi}_1$ as

$$H_0 = \begin{bmatrix} 0 & -1 & 0 \\ -1 & 0 & 1 \\ 0 & 1 & 0 \end{bmatrix}, \quad \vec{\psi}_1 = (1, -1, 1).$$

The corresponding flat band H_1 is

$$H_1 = \begin{bmatrix} 0.23624218 & 0.15535892 & -0.08088326 \\ -0.87350793 & -0.69073091 & 0.18277702 \\ 1.31303601 & 0.95651792 & -0.35651809 \end{bmatrix},$$
$$\vec{\psi}_2 = (3.14189192, -2.05220768, -0.94681365),$$
$$\vec{\psi}_3 = (1.08333333, -0.33333333, -0.41666667),$$
$$E_{\mathrm{FB}} = 0.5.$$

Example shown in Fig. 3(c). For the following input

$$H_0 = \begin{bmatrix} 0 & -1 & 2 \\ -1 & 0 & 1 \\ 2 & 1 & 0 \end{bmatrix}, \quad \vec{\psi}_1 = (1, -1, 1),$$

we find the flat band nearest-neighbor hopping matrix H_1:

$$H_1 = \begin{bmatrix} 0.06915801 & -0.66620419 & -0.7353622 \\ -0.31644957 & -0.3029663 & 0.01348327 \\ -0.46657738 & -0.38011423 & 0.08646314 \end{bmatrix},$$

$$\vec{\psi}_2 = (0.77717503, 2.50899893, 1.05355773),$$

$$\vec{\psi}_3 = (0.03571429, -0.57142857, 0.39285714),$$

$$E_{\mathrm{FB}} = 0.5.$$

Example shown in Fig. 3(d). The following input data

$$H_0 = \begin{bmatrix} 0 & 1 & 0 \\ 1 & 0 & 1 \\ 0 & 1 & 0 \end{bmatrix}, \quad \vec{\psi}_1 = (1, -1, 1)$$

provides an example of the flat band Hamiltonian, with the flat band being the ground state:

$$H_1 = \begin{bmatrix} -0.52279625 & 0.17024672 & 0.69304298 \\ -0.62702148 & -0.11461122 & 0.51241027 \\ -0.73124671 & -0.39946915 & 0.33177756 \end{bmatrix},$$

$$\vec{\psi}_2 = (0.25537008, 0.28652804, -0.59920373),$$

$$\vec{\psi}_3 = (0.25, -0.5, 0.25),$$

$$E_{\mathrm{FB}} = -1.5.$$

APPENDIX E: NETWORK CONSTRAINTS

We present here the details of the examples where the network connectivity was provided as an input to the FB generator. In all cases, one can find particular solutions to the resulting nonlinear system of equations.

Often network connectivity implies sparse H_0 and H_1 very sparse. Therefore inserting these sparse H_0 and H_1 into Eqs. (8)–(12) gives a set of equations that can be solved analytically. More precisely, as you will see in the examples below, when H_0 and H_1 are so sparse that the number unknowns (nonzero elements of H_1, H_0, and part of CLS) is less then or equal to the number of equations, we can solve Eqs. (8)–(12) analytically. Note that, instead of inserting H_1 and H_0 into Eqs. (8)–(12), we can get the same set of equations from Eq. (26) by zeroing the elements of h_1 corresponding to zero elements of H_1.

1. $U = 2$ case

a. 1D kagome

We consider the $d = 1$ version of the 2D kagome lattice. The nearest-neighbor Hamiltonian is restricted by the lattice connectivity to

$$H_0 = \begin{bmatrix} 0 & t_2 & 0 & 0 & 0 \\ t_2 & 0 & t_1 & 0 & 0 \\ 0 & t_1 & 0 & t_1 & 0 \\ 0 & 0 & t_1 & 0 & t_2 \\ 0 & 0 & 0 & t_2 & 0 \end{bmatrix}, \quad H_1 = \begin{bmatrix} 0 & t_1 & t_1 & 0 & 0 \\ 0 & 0 & 0 & 0 & 0 \\ 0 & 0 & 0 & 0 & 0 \\ 0 & 0 & 0 & 0 & 0 \\ 0 & 0 & t_1 & t_1 & 0 \end{bmatrix}.$$

The "*destructive interference*" condition (4), i.e., the last two equations in (15), implies that

$$\vec{\psi}_1 = (x_1, -x_2, x_2, -x_2, x_3), \quad \vec{\psi}_2 = (0, a, b, c, 0).$$

If we insert $\vec{\psi}_1$ and $\vec{\psi}_2$ above into Eqs. (15), we find

$$\begin{pmatrix} -x_2t_2 + (y_2 + y_3)t_1 \\ x_2t_1 + x_1t_2 \\ -2x_2t_1 \\ x_2t_1 + x_3t_2 \\ -x_2t_2 + (y_3 + y_4)t_1 \end{pmatrix} = E_{\mathrm{FB}} \begin{pmatrix} x_1 \\ -x_2 \\ x_2 \\ -x_2 \\ x_3 \end{pmatrix},$$

$$\begin{pmatrix} at_2 \\ (b + y_1)t_1 \\ (a + c + y_1 + y_5) \\ (b + y_5)t_1 \\ ct_2 \end{pmatrix} = E_{\mathrm{FB}} \begin{pmatrix} 0 \\ a \\ b \\ c \\ 0 \end{pmatrix}.$$

One the possible solutions of above equation is

$$a = c = 0,$$
$$t_1 = -\frac{E_{\mathrm{FB}}}{2},$$
$$t_2 = \frac{E_{\mathrm{FB}}}{2},$$
$$x_1 = -x,$$
$$x_2 = x,$$
$$x_3 = -x,$$
$$a = 0,$$
$$b = x,$$
$$c = 0.$$

This solution gives a flat band with energy E_{FB}. Thus the final solution is

$$\vec{\psi}_1 = (-x, -x, x, -x, -x),$$

$$\vec{\psi}_2 = (0, 0, x, 0, 0),$$

$$H_1 = \begin{bmatrix} 0 & -\frac{E_{\mathrm{FB}}}{2} & -\frac{E_{\mathrm{FB}}}{2} & 0 & 0 \\ 0 & 0 & 0 & 0 & 0 \\ 0 & 0 & 0 & 0 & 0 \\ 0 & 0 & 0 & 0 & 0 \\ 0 & 0 & -\frac{E_{\mathrm{FB}}}{2} & -\frac{E_{\mathrm{FB}}}{2} & 0 \end{bmatrix},$$

$$H_0 = \begin{bmatrix} 0 & \frac{E_{\mathrm{FB}}}{2} & 0 & 0 & 0 \\ \frac{E_{\mathrm{FB}}}{2} & 0 & -\frac{E_{\mathrm{FB}}}{2} & 0 & 0 \\ 0 & -\frac{E_{\mathrm{FB}}}{2} & 0 & -\frac{E_{\mathrm{FB}}}{2} & 0 \\ 0 & 0 & -\frac{E_{\mathrm{FB}}}{2} & 0 & \frac{E_{\mathrm{FB}}}{2} \\ 0 & 0 & 0 & \frac{E_{\mathrm{FB}}}{2} & 0 \end{bmatrix}.$$

This lattice has a flat band with flat band energy E_{FB}.

b. $U = 2$, $v = 3$ example

The connectivity of the network shown in Fig. 4(b) implies the following hopping matrices:

$$H_0 = \begin{pmatrix} 0 & t_1 & 0 \\ t_1 & 0 & t_2 \\ 0 & t_2 & 0 \end{pmatrix}, \quad H_1 = \begin{pmatrix} s_1 & s_2 & 0 \\ s_4 & s_5 & s_6 \\ 0 & s_7 & s_8 \end{pmatrix}.$$

We parametrize the CLS amplitudes as follows: $\vec{\psi}_1 = (x, y, z)$, $\vec{\psi}_2 = (a, b, c)$. Then Eqs. (15) gives

$$\begin{pmatrix} as_1 + bs_2 \\ as_4 + bs_5 + cs_6 \\ bs_7 + cs_8 \end{pmatrix} = \begin{pmatrix} xE_{\mathrm{FB}} - t_1 y \\ -t_1 x - t_2 z + yE_{\mathrm{FB}} \\ zE_{\mathrm{FB}} - t_2 y \end{pmatrix},$$
$$\begin{pmatrix} s_1 x + s_4 y \\ s_2 x + s_5 y + s_7 z \\ s_6 y + s_8 z \end{pmatrix} = \begin{pmatrix} aE_{\mathrm{FB}} - bt_1 \\ -at_1 + bE_{\mathrm{FB}} - ct_2 \\ cE_{\mathrm{FB}} - bt_2 \end{pmatrix},$$
$$\begin{pmatrix} s_1 x + s_2 y \\ s_4 x + s_5 y + s_6 z \\ s_7 y + s_8 z \end{pmatrix} = \begin{pmatrix} 0 \\ 0 \\ 0 \end{pmatrix},$$
$$\begin{pmatrix} as_1 + bs_4 \\ as_2 + bs_5 + cs_7 \\ bs_6 + cs_8 \end{pmatrix} = \begin{pmatrix} 0 \\ 0 \\ 0 \end{pmatrix}.$$

Here, H_0, E_{FB}, and $\vec{\psi}_1$ as free parameters. If we fix $x = 1$, $y = 2$, $z = 1$, $t_1 = 1$, $t_2 = 2$, $E_{\mathrm{FB}} = 3$, then we find one particular solution of above equations:

$$s_1 = \frac{2\sqrt{2}}{3}, \quad s_2 = -\frac{\sqrt{2}}{3},$$
$$s_4 = \frac{2\sqrt{2}}{3}, \quad s_5 = \frac{\sqrt{2}}{3},$$
$$s_6 = -\frac{1}{3}(4\sqrt{2}), \quad s_7 = -\frac{\sqrt{2}}{3},$$
$$s_8 = \frac{2\sqrt{2}}{3}, \quad a = \frac{1}{\sqrt{2}},$$
$$b = -\frac{1}{\sqrt{2}}, \quad c = -\sqrt{2},$$

from which follow the hopping matrices and the CLS amplitudes

$$H_0 = \begin{pmatrix} 0 & 1 & 0 \\ 1 & 0 & 2 \\ 0 & 2 & 0 \end{pmatrix}, \quad H_1 = \begin{pmatrix} \frac{2\sqrt{2}}{3} & -\frac{\sqrt{2}}{3} & 0 \\ \frac{2\sqrt{2}}{3} & \frac{\sqrt{2}}{3} & -\frac{1}{3}(4\sqrt{2}) \\ 0 & -\frac{\sqrt{2}}{3} & \frac{2\sqrt{2}}{3} \end{pmatrix},$$
$$\vec{\psi}_1 = (1, 2, 1), \quad \vec{\psi}_2 = \left(\frac{1}{\sqrt{2}}, -\frac{1}{\sqrt{2}}, -\sqrt{2}\right).$$

2. $U = 3$ case

a. $U = 3$, $v = 3$ example

We consider networks shown in Fig. 4(c). Its connectivity requires the following hopping matrices

$$H_0 = \begin{pmatrix} 0 & t_1 & 0 \\ t_1 & 0 & t_2 \\ 0 & t_2 & 0 \end{pmatrix}, \quad H_1 = \begin{pmatrix} s_1 & s_1 & 0 \\ -\frac{s_1}{2} & -\frac{s_1}{2} - s_6 & s_6 \\ 0 & 2s_6 & -2s_6 \end{pmatrix}.$$

According to "*destructive interference*" condition (4), we parametrize $\vec{\psi}_1$, $\vec{\psi}_2$, $\vec{\psi}_3$ as follows:

$$\vec{\psi}_1 = (-y, y, y), \quad \vec{\psi}_2 = (a, b, c), \quad \vec{\psi}_3 = (d, 2d, d).$$

Then the main equations (24) become

$$\begin{pmatrix} (a+b)s_1 \\ (c-b)s_6 - \frac{1}{2}(a+b)s_1 \\ 2(b-c)s_6 \end{pmatrix} = \begin{pmatrix} -y(E_{\mathrm{FB}} + t_1) \\ y(E_{\mathrm{FB}} + t_1 - t_2) \\ y(E_{\mathrm{FB}} - t_2) \end{pmatrix},$$
$$\begin{pmatrix} \frac{3}{2}(2d-y)s_1 \\ (y-d)s_6 - \frac{3}{2}(d+y)s_1 \\ (2d-y)s_6 \end{pmatrix} = \begin{pmatrix} aE_{\mathrm{FB}} - bt_1 \\ bE_{\mathrm{FB}} - at_1 - ct_2 \\ cE_{\mathrm{FB}} - bt_2 \end{pmatrix},$$
$$\begin{pmatrix} \frac{1}{2}(2a-b)s_1 \\ \left(a - \frac{b}{2}\right)s_1 - (b-2c)s_6 \\ (b-2c)s_6 \end{pmatrix} = \begin{pmatrix} d(E_{\mathrm{FB}} - 2t_1) \\ d(2E_{\mathrm{FB}} - t_1 - t_2) \\ d(E_{\mathrm{FB}} - 2t_2) \end{pmatrix}.$$

Again the above system admits many solutions. We pick one with $t_1 = 1$, $t_2 = 2$, $b = \frac{1}{2}$, and

$$a = \frac{1}{80}(3\sqrt{21} + 23), \quad c = \frac{1}{80}(\sqrt{21} + 41),$$
$$d = \frac{1}{40}\left(-7\sqrt{\frac{3}{2}} - \sqrt{\frac{7}{2}}\right), \quad y = \frac{1}{40}\left(\sqrt{\frac{3}{2}} + 3\sqrt{\frac{7}{2}}\right),$$
$$E_{\mathrm{FB}} = \frac{5}{2}, \quad s_1 = -\frac{\sqrt{\frac{7}{2}}}{3}, \quad s_6 = -\frac{\sqrt{\frac{3}{2}}}{2}.$$

Therefore the CLS amplitudes and the hopping matrices are

$$\vec{\psi}_1 = \begin{pmatrix} \frac{1}{40}\left(-\sqrt{\frac{3}{2}} - 3\sqrt{\frac{7}{2}}\right) \\ \frac{1}{40}\left(\sqrt{\frac{3}{2}} + 3\sqrt{\frac{7}{2}}\right) \\ \frac{1}{40}\left(\sqrt{\frac{3}{2}} + 3\sqrt{\frac{7}{2}}\right) \end{pmatrix},$$
$$\vec{\psi}_2 = \begin{pmatrix} \frac{1}{80}(3\sqrt{21} + 23) \\ \frac{1}{2} \\ \frac{1}{80}\left(\sqrt{21} + 41\right) \end{pmatrix},$$
$$\vec{\psi}_3 = \begin{pmatrix} \frac{1}{40}\left(-7\sqrt{\frac{3}{2}} - \sqrt{\frac{7}{2}}\right) \\ \frac{1}{20}\left(-7\sqrt{\frac{3}{2}} - \sqrt{\frac{7}{2}}\right) \\ \frac{1}{40}\left(-7\sqrt{\frac{3}{2}} - \sqrt{\frac{7}{2}}\right) \end{pmatrix},$$
$$H_1 = \begin{pmatrix} -\frac{\sqrt{\frac{7}{2}}}{3} & -\frac{\sqrt{\frac{7}{2}}}{3} & 0 \\ \frac{\sqrt{\frac{7}{2}}}{6} & \frac{\sqrt{\frac{3}{2}}}{2} + \frac{\sqrt{\frac{7}{2}}}{6} & -\frac{\sqrt{\frac{3}{2}}}{2} \\ 0 & -\sqrt{\frac{3}{2}} & \sqrt{\frac{3}{2}} \end{pmatrix},$$
$$H_0 = \begin{pmatrix} 0 & 1 & 0 \\ 1 & 0 & 2 \\ 0 & 2 & 0 \end{pmatrix},$$

which gives a flat band with energy $E_{\mathrm{FB}} = 5/2$. Schematics and the band structure of this lattice is shown in Fig. 4(c).

[1] O. Derzhko, J. Richter, and M. Maksymenko, Strongly correlated flat-band systems: The route from Heisenberg spins to hubbard electrons, Int. J. Mod. Phys. B **29**, 1530007 (2015).

[2] D. Leykam, A. Andreanov, and S. Flach, Artificial flat band systems: From lattice models to experiments, Adv. Phys.: X **3**, 1473052 (2018).

[3] D. Leykam and S. Flach, Perspective: Photonic flatbands, APL Photonics **3**, 070901 (2018).

[4] O. Derzhko and J. Richter, Universal low-temperature behavior of frustrated quantum antiferromagnets in the vicinity of the saturation field, Eur. Phys. J. B **52**, 23 (2006).

[5] O. Derzhko, J. Richter, A. Honecker, M. Maksymenko, and R. Moessner, Low-temperature properties of the Hubbard model on highly frustrated one-dimensional lattices, Phys. Rev. B **81**, 014421 (2010).

[6] M. Hyrkäs, V. Apaja, and M. Manninen, Many-particle dynamics of bosons and fermions in quasi-one-dimensional flat-band lattices, Phys. Rev. A **87**, 023614 (2013).

[7] A. Mielke, Ferromagnetism in the hubbard model on line graphs and further considerations, J. Phys. A: Math. Gen. **24**, 3311 (1991).

[8] H. Tasaki, Ferromagnetism in the Hubbard Models with Degenerate Single-Electron Ground States, Phys. Rev. Lett. **69**, 1608 (1992).

[9] T. Misumi and H. Aoki, New class of flat-band models on tetragonal and hexagonal lattices: Gapped versus crossing flat bands, Phys. Rev. B **96**, 155137 (2017).

[10] S. Nishino and M. Goda, Three-dimensional flat-band models, J. Phys. Soc. Jpn. **74**, 393 (2005).

[11] E. H. Lieb, Two Theorems on the Hubbard Model, Phys. Rev. Lett. **62**, 1201 (1989).

[12] A. Mielke, Ferromagnetic ground states for the Hubbard model on line graphs, J. Phys. A: Math. Gen. **24**, L73 (1991).

[13] A. Mielke, Exact results for the u = infinity Hubbard model, J. Phys. A: Math. Gen. **25**, 6507 (1992).

[14] U. Brandt and A. Giesekus, Hubbard and Anderson Models on Perovskitelike Lattices: Exactly Solvable Cases, Phys. Rev. Lett. **68**, 2648 (1992).

[15] A. Ramachandran, A. Andreanov, and S. Flach, Chiral flat bands: Existence, engineering, and stability, Phys. Rev. B **96**, 161104 (2017).

[16] D. Guzmán-Silva, C. Mejía-Cortés, M. A. Bandres, M. C. Rechtsman, S. Weimann, S. Nolte, M. Segev, A. Szameit, and R. A. Vicencio, Experimental observation of bulk and edge transport in photonic lieb lattices, New J. Phys. **16**, 063061 (2014).

[17] R. A. Vicencio, C. Cantillano, L. Morales-Inostroza, B. Real, C. Mejía-Cortés, S. Weimann, A. Szameit, and M. I. Molina, Observation of Localized States in Lieb Photonic Lattices, Phys. Rev. Lett. **114**, 245503 (2015).

[18] S. Mukherjee and R. R. Thomson, Observation of localized flat-band modes in a quasi-one-dimensional photonic rhombic lattice, Opt. Lett. **40**, 5443 (2015).

[19] S. Weimann, L. Morales-Inostroza, B. Real, C. Cantillano, A. Szameit, and R. A. Vicencio, Transport in sawtooth photonic lattices, Opt. Lett. **41**, 2414 (2016).

[20] S. Xia, Y. Hu, D. Song, Y. Zong, L. Tang, and Z. Chen, Demonstration of flat-band image transmission in optically induced lieb photonic lattices, Opt. Lett. **41**, 1435 (2016).

[21] S. Taie, H. Ozawa, T. Ichinose, T. Nishio, S. Nakajima, and Y. Takahashi, Coherent driving and freezing of bosonic matter wave in an optical lieb lattice, Sci. Adv. **1**, e1500854 (2015).

[22] G.-B. Jo, J. Guzman, C. K. Thomas, P. Hosur, A. Vishwanath, and D. M. Stamper-Kurn, Ultracold Atoms in a Tunable Optical Kagome Lattice, Phys. Rev. Lett. **108**, 045305 (2012).

[23] N. Masumoto, N. Y. Kim, T. Byrnes, K. Kusudo, A. Löffler, S. Höfling, A. Forchel, and Y. Yamamoto, Exciton-polariton condensates with flat bands in a two-dimensional kagome lattice, New J. Phys. **14**, 065002 (2012).

[24] F. Baboux, L. Ge, T. Jacqmin, M. Biondi, E. Galopin, A. Lemaître, L. Le Gratiet, I. Sagnes, S. Schmidt, H. E. Türeci, A. Amo, and J. Bloch, Bosonic Condensation and Disorder-Induced Localization in a Flat Band, Phys. Rev. Lett. **116**, 066402 (2016).

[25] A. Mielke and H. Tasaki, Ferromagnetism in the hubbard model, Commun. Math. Phys. **158**, 341 (1993).

[26] H. Tasaki, Hubbard model and the origin of ferromagnetism, Eur. Phys. J. B **64**, 365 (2008).

[27] H. Tasaki, Stability of Ferromagnetism in the Hubbard Model, Phys. Rev. Lett. **73**, 1158 (1994).

[28] M. Maksymenko, A. Honecker, R. Moessner, J. Richter, and O. Derzhko, Flat-Band Ferromagnetism As a Pauli-Correlated Percolation Problem, Phys. Rev. Lett. **109**, 096404 (2012).

[29] D. Leykam, J. D. Bodyfelt, A. S. Desyatnikov, and S. Flach, Localization of weakly disordered flat band states, Eur. Phys. J. B **90**, 1 (2017).

[30] J. D. Bodyfelt, D. Leykam, C. Danieli, X. Yu, and S. Flach, Flatbands Under Correlated Perturbations, Phys. Rev. Lett. **113**, 236403 (2014).

[31] C. Danieli, J. D. Bodyfelt, and S. Flach, Flat-band engineering of mobility edges, Phys. Rev. B **91**, 235134 (2015).

[32] R. Khomeriki and S. Flach, Landau-Zener Bloch Oscillations with Perturbed Flat Bands, Phys. Rev. Lett. **116**, 245301 (2016).

[33] C. Danieli, A. Maluckov, and S. Flach, Compact discrete breathers on flat-band networks, Low Temp. Phys. **44**, 678 (2018).

[34] M. Johansson, U. Naether, and R. A. Vicencio, Compactification tuning for nonlinear localized modes in sawtooth lattices, Phys. Rev. E **92**, 032912 (2015).

[35] B. Real and R. A. Vicencio, Controlled mobility of compact discrete solitons in nonlinear lieb photonic lattices, Phys. Rev. A **98**, 053845 (2018).

[36] A. Mielke, Pair formation of hard core bosons in flat band systems, J. Stat. Phys. **171**, 679 (2018).

[37] S. Peotta and P. Törmä, Superfluidity in topologically nontrivial flat bands, Nat. Commun. **6**, 8944 (2015).

[38] A. Julku, S. Peotta, T. I. Vanhala, D.-H. Kim, and P. Törmä, Geometric Origin of Superfluidity in the Lieb-Lattice Flat Band, Phys. Rev. Lett. **117**, 045303 (2016).

[39] R. G. Dias and J. D. Gouveia, Origami rules for the construction of localized eigenstates of the hubbard model in decorated lattices, Sci. Rep. **5**, 16852 (2015).

[40] L. Morales-Inostroza and R. A. Vicencio, Simple method to construct flat-band lattices, Phys. Rev. A **94**, 043831 (2016).

[41] M. Röntgen, C. V. Morfonios, and P. Schmelcher, Compact localized states and flat bands from local symmetry partitioning, Phys. Rev. B **97**, 035161 (2018).

[42] S. Nishino, M. Goda, and K. Kusakabe, Flat bands of a tight-binding electronic system with hexagonal structure, J. Phys. Soc. Jpn. **72**, 2015 (2003).

[43] S. Flach, D. Leykam, J. D. Bodyfelt, P. Matthies, and A. S. Desyatnikov, Detangling flat bands into fano lattices, Europhys. Lett. **105**, 30001 (2014).

[44] W. Maimaiti, A. Andreanov, H. C. Park, O. Gendelman, and S. Flach, Compact localized states and flat-band generators in one dimension, Phys. Rev. B **95**, 115135 (2017).

[45] R. Mondaini, G. G. Batrouni, and B. Grémaud, Pairing and superconductivity in the flat band: Creutz lattice, Phys. Rev. B **98**, 155142 (2018).

[46] G. Gligorić, P. P. Beličev, D. Leykam, and A. Maluckov, Nonlinear symmetry breaking of aharonov-bohm cages, Phys. Rev. A **99**, 013826 (2019).

[47] M. Tovmasyan, S. Peotta, L. Liang, P. Törmä, and S. D. Huber, Preformed pairs in flat bloch bands, Phys. Rev. B **98**, 134513 (2018).

[48] M. Tovmasyan, S. Peotta, P. Törmä, and S. D. Huber, Effective theory and emergent SU(2) symmetry in the flat bands of attractive hubbard models, Phys. Rev. B **94**, 245149 (2016).

[49] M. Tovmasyan, E. P. L. van Nieuwenburg, and S. D. Huber, Geometry-induced pair condensation, Phys. Rev. B **88**, 220510 (2013).

[50] S. Longhi, Photonic flat-band laser, Opt. Lett. **44**, 287 (2019).

[51] I. Vakulchyk, M. V. Fistul, P. Qin, and S. Flach, Anderson localization in generalized discrete-time quantum walks, Phys. Rev. B **96**, 144204 (2017).

[52] E. Travkin, F. Diebel, and C. Denz, Compact flat band states in optically induced flatland photonic lattices, Appl. Phys. Lett. **111**, 011104 (2017).

[53] D. Boley and G. H. Golub, A survey of matrix inverse eigenvalue problems, Inv. Probl. **3**, 595 (1987).

[54] C. Poli, H. Schomerus, M. Bellec, U. Kuhl, and F. Mortessagne, Partial chiral symmetry-breaking as a route to spectrally isolated topological defect states in two-dimensional artificial materials, 2D Mat. **4**, 025008 (2017).

[55] L. Ge, Non-hermitian lattices with a flat band and polynomial power increase [invited], Photon. Res. **6**, A10 (2018).

[56] D. Leykam, S. Flach, and Y. D. Chong, Flat bands in lattices with non-hermitian coupling, Phys. Rev. B **96**, 064305 (2017).

[57] L. Ge, Parity-time symmetry in a flat-band system, Phys. Rev. A **92**, 052103 (2015).

[58] A. Ben-Israel and T. N. E. Greville, *Generalized Inverses: Theory and Applications* (Springer Science & Business Media, New York, 2003), Vol. 15.